Geomechanics and Engineering, *Vol. 11, No. 2 (2016) 177-195*
DOI: http://dx.doi.org/10.12989/gae.2016.11.2.177

Experimental evaluation of the active tension bolt

Sang-Hwan Kim [1a], Ki-Il Song [*2] and Jae-Hyun Park [3b]

[1] *Hoseo University, Department of Civil Engineering, 20, Hoeo-ro 79 Beon-gil, Baebang-eup, Asan-si, 31499, Republic of Korea*
[2] *Inha University, Department of Civil Engineering,100 Inha-ro, Nam-gu, Incheon, 22212, Republic of Korea*
[3] *Hankook 2 Arch, 78 Jangmi-ro, Bundang-gu, Seongnam-si, Gyeonggi-do, 13496, Republic of Korea*

(*Received September 03, 2016, Revised March 24, 2016, Accepted April 20, 2016*)

Abstract. To secure the stability of geotechnical infrastructures and minimize failures during the construction process, a number of support systems have been introduced in the last several decades. In particular, stabilization methods using steel bars have been widely used in the field of geotechnical engineering. Rock bolt system is representative support system using steel bars. Pre-stressing has been applied to enhance reinforcement performance but can be released because of the failure of head or anchor sections. To overcome this deficiency, this paper proposes an innovative support system that can actively reinforce the weak ground along the whole structural element by introducing an active tension bolt containing a spring unit to the middle of the steel bar to increase its reinforcement capacity. In addition, the paper presents the support mechanism of the active tension bolt based on a theoretical study and employs an experimental study to validate the performance of the proposed active tension bolt based on a down-scaled model. To examine the feasibility of the active tension unit in a pillar, the paper considers a pullout test and a small-scale experimental model. The experimental results suggest the active tension bolt to be an effective support system for pillar reinforcement.

Keywords: active tension bolt; tunnel pillar reinforcement; support mechanism; experimental study

1. Introduction

Because of rapid economic growth, there has been a sharp increase in the number of geotechnical infrastructure construction projects such as slopes and tunnels in urban areas. Construction sites in urban areas are confined by existing infrastructures and public structures (Franzius *et al*. 2004). Therefore, various support systems have been employed to stabilize geotechnical infrastructures and minimize failures during the construction process. In particular, stabilization methods using steel bars have been widely used in the field of geotechnical engineering.

Rock bolts represent a primary support system in tunnels based on the new Austrian tunneling method. Rock bolts have been widely adopted as primary tunnel support systems using various types of steel products (Siad 2001, Osgouiand Ü nal 2009, Blanco-Fernandez *et al*. 2011, Divi *et al*.

∗Corresponding author, Lecturer, E-mail: ksong@inha.ac.kr
[a] Professor, E-mail: kimsh@hoseo.edu
[b] Director, E-mail: 2archboss@hanmail.net

http://www.techno-press.org/?journal=gae&subpage=7 ISSN: 2005-307X (Print), 2092-6219 (Online)

2011, Song *et al*. 2013). Rock bolt uses steel reinforcements to increase shear strength, and tensile strength. Rock bolt binds together a fractured and jointed rock mass and act as a composite beam. Rock bolt can be combined with shotcrete and a wire mesh to increase the shear strength of the overall ground and minimize ground movements during and after construction.

Many studies have considered the use of steel bars to reinforce geotechnical infrastructures in recent years, including the development of new types of support systems using steel bars (Ansell 2005), the development of evaluation techniques for rock bolt support systems (Lee *et al*., 2012), theoretical and numerical analyses of support mechanisms (Li and Stillborg 1999, Komurlu and Kesimal 2015, Livaoglu 2013, Mahdi and Katebi 2015, Lin *et al*. 2015), and the development of advanced materials that can enhance performance.

Support systems composed of steel bars and grout not only strengthens or stabilizes a jointed rock mass, but also has a marked effect on the rock mass stiffness (Chappell 1989). Pre-stressing is applied to enhance the performance of such support systems. The design and construction of anchor bolts are standardized in many standard codes such as the AISC (2006), the ACI (1976), and the Eurocode (2005) for the static stress of traction and/or shearing. Pre-stress can be secured by two-speed resin bonded rock bolt system during the construction (Spearing *et al*. 2011). However, release of pre-stress can be caused not only by the failure of the head or anchor section but also by fracture of steel bar and deterioration since mechanical characteristics of structural materials change over time (Pells and Bertuzzi 1999, Delhomme *et al*. 2010). In critical conditions, the whole support structure can lose its reinforcement function. When steel bars are used for temporary support, machines can be damaged during the removal process. These limitations of support systems can increase construction costs and reduce the stability of geotechnical infrastructures. In this regard, there is a need to develop an innovative support system using steel bars to enhance its performance and efficiency.

This paper proposes an active tension bolt containing a spring unit to increase the reinforcement capacity and durability. The paper presents the support mechanism of the active tension bolt through a theoretical study and employs an experimental test to validate the performance of the proposed active tension bolt based on a down-scaled tension unit using the active tension bolt to reinforce the pillar. In addition, the paper considers pullout test and a small-scale experimental model to evaluate the practical applicability of the active tension bolt.

2. The development of the active tension bolt

2.1 The support mechanism of the active tension bolt

The efficiency and performance of support systems using steel bars or steel pipes combined with grouting in tunnels and slopes are influenced by the quality and regularity of grouting (Lee *et al*. 2012). To improve the quality of support systems, various structural shapes of steel bars have been developed, and various types of grouting materials have been employed to fill drilled holes (Song *et al*. 2010, Blanco Martín *et al*. 2011, Chen *et al*. 2013). Although a steel bar is inherently highly stiff, its long-term performance can be affected by corrosion and local failures induced by a fracture opening (Jiang *et al*. 2014). In such a case, the long-term stability of geotechnical infrastructures can be affected by the failure of the bolt support system (Pells and Bertuzzi 1999).

The typical structure of a support system using steel bars is accompanied by grouting after the insertion of steel bars into the drilled hole. Recently, tension or pre-stress has been applied to

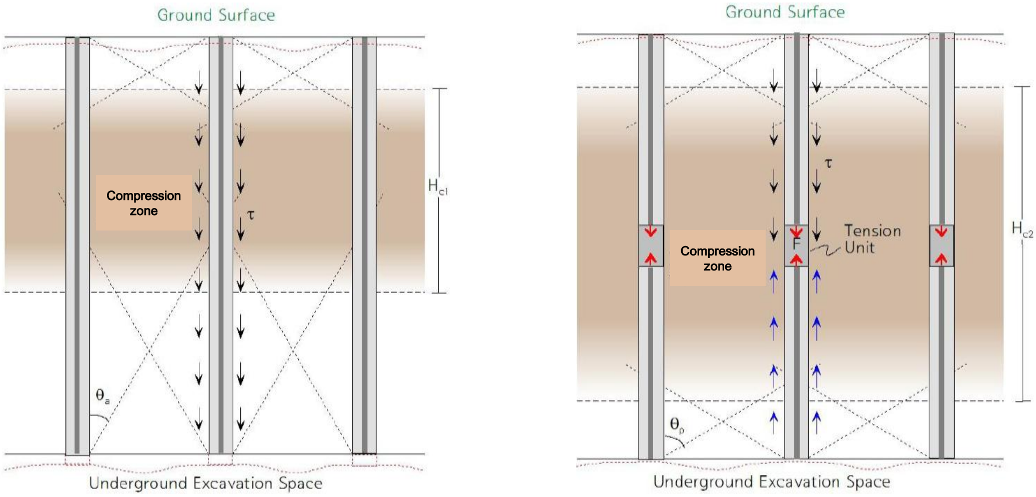

(a) (b)

Fig. 1 The thickness of the compressed zone and the direction of mobilized skin friction in: (a) the general bolt system; and (b) the active tension bolt system (note: H_{c1} is the thickness of the compression zone from a conventional rock bolt system, and H_{c2} is that from an active tension bolt system)

enhance support strength. However, the failure of steel induced by corrosion, the separation of the steel-grouting interface, and local fractures during the operation can reduce the performance of the overall support system and cause stability problems. To overcome the limitations of conventional support systems using steel bars, this paper proposes an active tension unit that can maintain its performance even after a local failure.

To develop the support mechanism, grout in the drilled hole and steel bars are assumed to be elastic and fully integrated. Although the load transfer mechanism along the axially loaded grouted bar is highly complicated and peak bond stress shifts during its progressive failure (Li and Stillborg 1999), it can be simplified that the frictional shear strength between grout and ground can be considered as a representative element of shear resistance along the active tension bolt.

The compressed zone developed by the active tension bolt is wider than that for the general bolt system. As shown in Fig. 1, skin friction is mobilized along a single direction in the general bolt system. However, the elongated tension unit contracts two neighboring steel bar segments and mobilizes skin friction in two directions.

H_{c1} and H_{c2} define the thicknesses of compression zone. In this study, it is assumed that the excavation surface shows active and passive failure due to excavation. When the active tension is not introduced, the excavation surface shows active failure and the angle of failure plane is governed by active state (θ_a). When active tension is introduced, the excavation surface shows passive failure and the angle of failure plane is governed by passive state (θ_p).Therefore, the arching (compression) zone induced by the active tension bolt is thicker than that for the general bolt system (i.e., $H_{c1} < H_{c2}$). This implies that the active tension bolt can carry higher earth pressure in soil.

The load transfer mechanism induced by the tension unit in the active tension bolt is shown in Fig. 2. This mechanism can change depending on the number of tension units and the length of the steel bar segment. If a single tension unit is implemented in the active tension bolt, the ground near

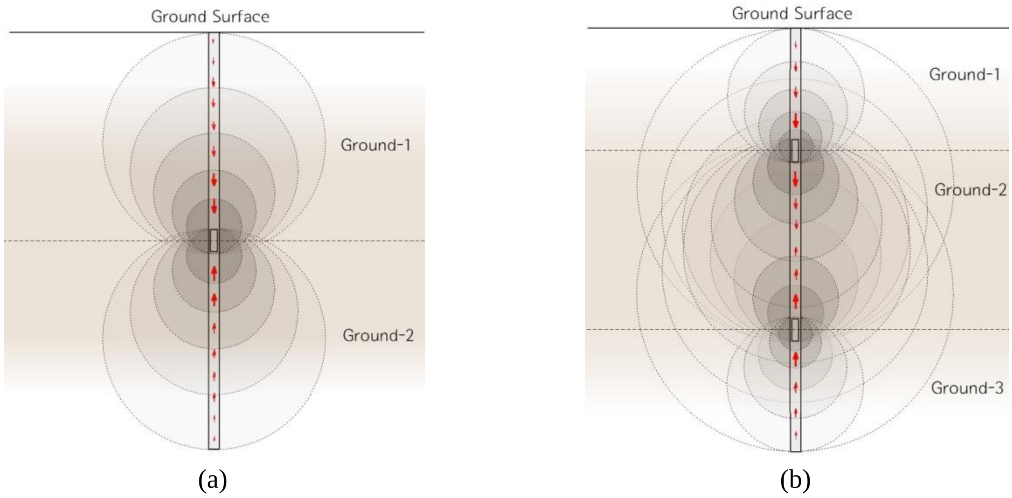

Fig. 2 The load transfer mechanism along the active tension bolt with: (a) a single tension unit; and (b) a dual tension unit

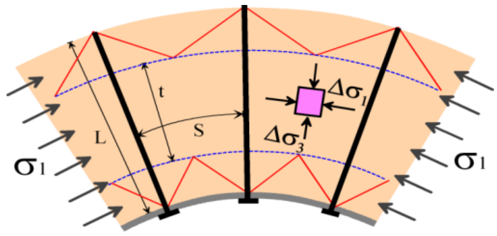

Fig. 3 The stress distribution in the reinforced zone with the active tension bolt

the tension unit contracts and forms an arching zone, as shown in Fig. 2(a). If the ground beneath the active tension bolt is excavated, then the displacement induced by the excavation can be reduced because of the arching effect of the load transfer mechanism.

If the active tension bolt includes two tension units, then the influential area affected by the tension unit is reduced, and the density of the compression force distribution increases. Therefore, the ground near each tension unit contracts more and forms a wider arching zone, as shown in Fig. 2(b). In this case, the ground is supported by the higher tensile force, and there is a significant decrease in the displacement induced by the excavation. According to study done by Zhao *et al*. (2013) and Petros (1991), pre-stress introduced bolt creates active arch in the ground around it and this arch makes the excavated space self-supported.

The maximum principal stress developed in the reinforced zone can be shown as Fig. 3. This stress increases along the active tension bolt, and its increment ($\Delta\sigma_1$) induced by the tension bolt with spacing s can be derived as follows

$$\Delta\sigma_1 = tan^2\left(45 + \frac{\phi}{2}\right)\Delta\sigma_3 = tan^2\left(45 + \frac{\phi}{2}\right)\frac{p}{s^2} \quad (1)$$

where p is the support pressure of the tension unit, ϕ is the friction angle, and $\Delta\sigma_3$ is the increment

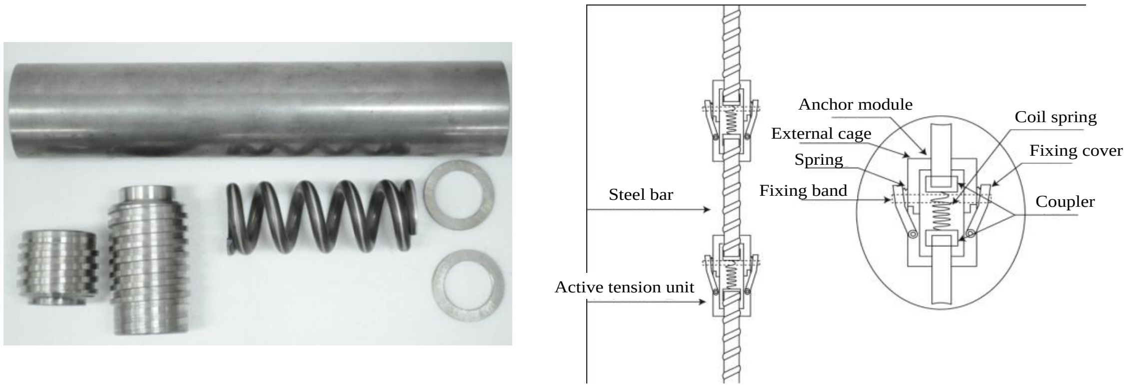

(a) (b)

Fig. 4 An active tension unit: (a) components of a tension unit; and (b) the specification of the active tension bolt

of the minimum principal stress.

In summary, the addition of the spring to a bolt permits stiffer response of sections of the bolt to the applied tension such that the tensile loading is applied along the whole length of the bolt, thereby engaging the sections of the bolt where the springs are located.

2.2 The structure of the active tensioning module

The active tension bolt is composed mainly of steel bars and a number of active tension units. An active tension unit is composed of coil springs, couplers, external cages, fixing bands, and fixing covers. Fig. 4(a) presents an active tension unit's components, and Fig. 4(b) shows the schematic design of the active tension bolt combined with a tension unit.

A coil spring is attached to couplers fixed at the end of steel bars. External cages insulate couplers and coil springs and protect the system from grout. A hinge-type fixing cover is attached to the external cage, and a spring is installed between the fixing cover and the external cage. The fixing band rotates to confine the fixing cover and separate external cages. The fixing cover plays a role as an anchor when the drilled hole is fully grouted. Mechanical interlocking will be created by fixing cover after the drilled hole is fully grouted. Multiple steel bar segments can be connected by several tension units in a single set of active tension bolts. The springs are stretched during installation, and then permitted to contract after the grout is installed, then there will be active tension applied along the tension bolt.

The type of bar material can be changed according to the application purpose. For the bolt support system in a tunnel, for example, glass-fiber reinforced plastic (GFRP) can be used as the main support material. GFRP can carry high-tensile stress, and the axial force can support tunnels with tension units.

3. The performance of the active tension bolt

3.1 The experimental setup

To evaluate the performance of the active tension bolt, an experimental study was conducted.

The properties of the spring, the main component of the active tension unit, were determined through a simple loading test. A pullout test with the active tension bolt was conducted in a chamber. Based on a series of pullout tests, the performance of the active tension bolt was assessed.

3.1.1 The determination of spring properties

To examine the stiffness and elastic limit of the spring, a simple loading test was conducted with a steel spring. In this study, the spring constant was obtained for an industrial spring used in the experimental study. In terms of the industrial spring's physical properties, length, thickness of coil, and outer diameter of spring were 18 mm, 0.7 mm, and 8 mm, respectively.

To obtain the load-displacement relationship, a pullout test setup was adopted. The linear load-displacement relationship was determined based on the results (Fig. 5(a)). Based on the test results, the spring constant for the industrial spring used in this active tension unit was determined as 0.5 N/mm. However, this spring constant (K) is valid only under 15 Newtons.

If the stress is sufficiently low, then the solid recovers its original shape and volume when the load is removed. However, if the stress increases and exceeds some elastic limit, then the material shows some permanent displacement even after the stress is removed. To prevent any plastic deformation and maintain the elastic condition during the experimental test, the elastic limit of the industrial spring was examined.

As shown in Fig. 5(b), the load-displacement curve was obtained. The region showing a linear load-displacement behavior can be considered the elastic limit. As shown in Fig. 5(b), the maximum available load of the industrial spring was 33-35 Newtons.

3.1.2 The pullout test of the steel bar

The formation of homogeneous sand ground in a chamber is a key factor in an experimental study, and the relative density of sand in a chamber should be uniform. In this study, the sand ground was prepared using the raining method, and Jumunjin sand was used. Fig. 6 shows the particle size distribution of Jumunjin sand. Here 91% of the sand particles passed the No. 40 sieve (sieve size = 0.425 mm), and the coefficient of uniformity was 1.47. In this regard, the sand particle was considered to have a uniform distribution and classified as SP based on the unified soil classification system.

To form a uniform sand ground sample in the chamber, a preliminary study was conducted to determine the falling height and the travel time to achieve the aimed relative density. The dry unit weight of the sand ground was controlled for Loose sand ground (dry unit weight = 13.6 kN/m^3)

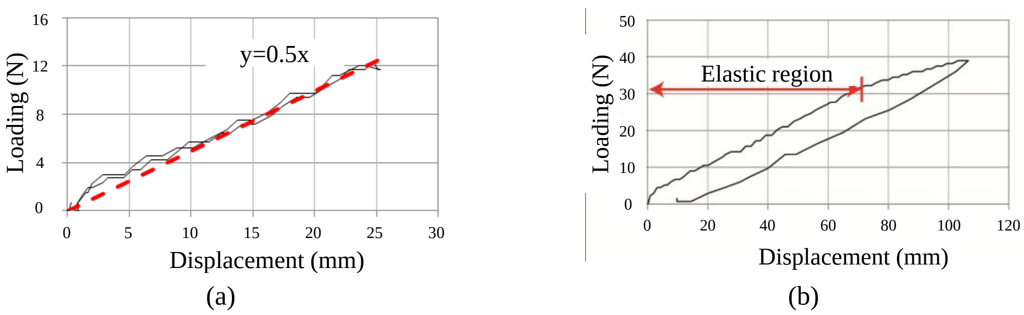

Fig. 5 The load-displacement relationship of the industrial spring: (a) the determination of the spring constant; and (b) the determination of the elastic limit

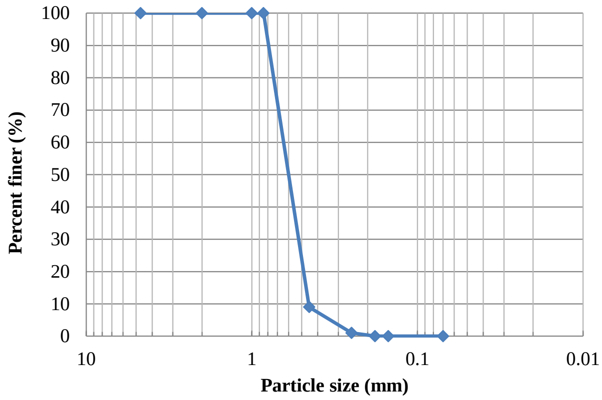

Fig. 6 The particle size distribution of Jumunjin sand

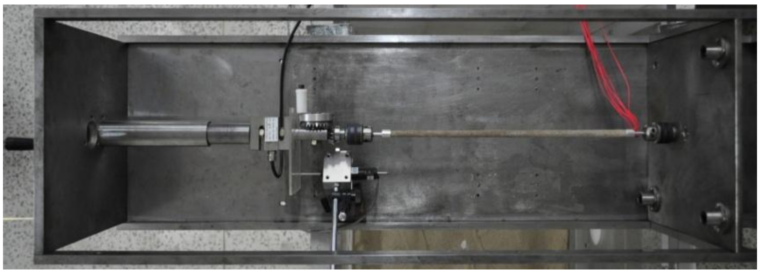

(a)

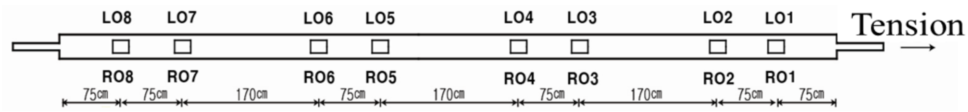

(b)

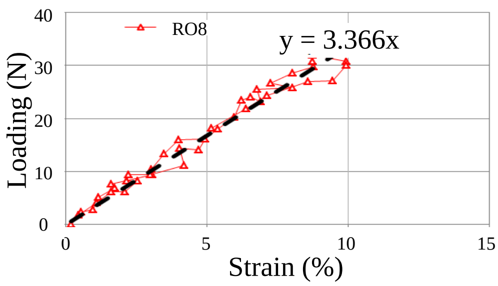

(c)

Fig. 7 The pullout test setup to obtain the stress-strain curve: (a) a 480 mm rod in a chamber; (b) the location of the strain gauge on the rod; and (c) the stress-strain curve of the rod at RO8

and dense sand ground (dry unit weight = 15.9 kN/m^3) were selected as representative ground conditions. The relative density of the loose sand ground and that of the dense sand ground were 17.9% and 81.9%, respectively. Earth pressure at the center of the chamber was monitored to validate the uniform stress distribution.

The stress-strain behavior of the material used in the study was obtained from the pullout test set (Fig. 7(a)). To obtain the reasonable stress-strain behavior, the rod length was changed. However, the diameter of the rod was fixed to 6 cm in all experiments. Because of the capacity of the spring, 3 kg was considered the maximum load that could be imposed on the tension unit. Strain gages were attached to the rod, as shown in Fig. 7(b). To model the pullout test in sand, the rod was completely embedded in the sand during the experiment. Fig. 7(c) shows the representative load-strain curve obtained from the pullout test. The rod showed an elastic behavior under the working load (3 kg).

3.2 The pullout test with the active tension bolt

An experimental study was conducted to investigate the performance of the active tension bolt. A total of 18 cases were examined. Tables 2, 3, and 4 summarize these cases. To examine the performance of the active tension bolt under different ground conditions, loose and dense sand ground samples were considered. In addition, the surcharge was varied from 60 kg to 120 kg. To investigate the effect of the number of tension units on the stress-strain behavior, single and dual tension units were added to the middle of the rod. The pullout test for the rod without the active tension unit was conducted as a control. Fig. 8 shows the location of the strain gauge and the tension unit for the active tension bolt with single and dual tension units and for the control, respectively. Fig. 9 shows the test setup for the aforementioned cases.

The results of the pullout test are similar to those in Fig. 7(c). The peak load and the corresponding strain can be obtained from the load-strain relationship. Tables 1, 2, and 3 show the experimental results for models without a tension unit, with a single tension unit, and with a dual tension unit, respectively. Two tests were conducted for each case, and the results were averaged. Fig. 10 shows the mobilized modulus of the active tension bolt based on the surcharge and the ground condition.

The modulus obtained from dense sand was higher than that obtained from loose sand. This trend was found in the other cases. Inter-particle friction and interlocking effects in dense sand

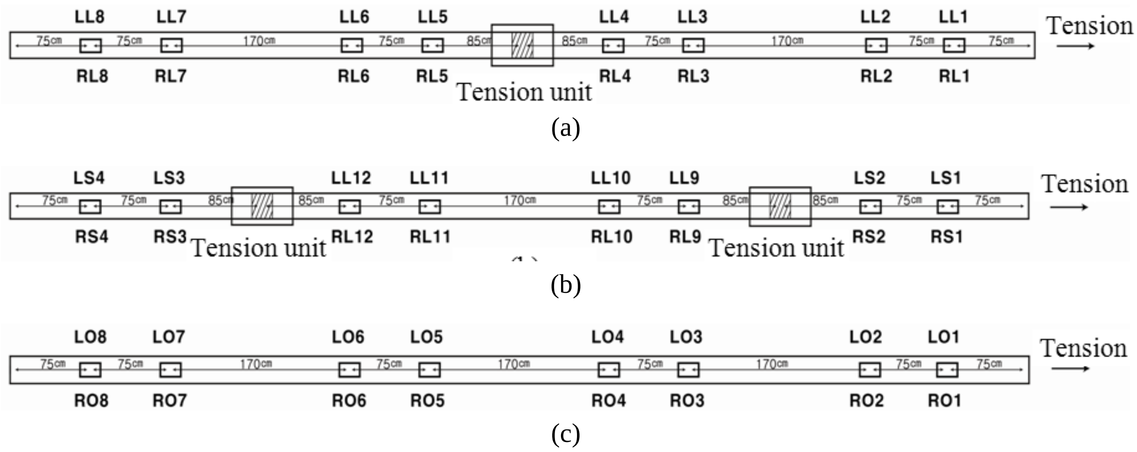

Fig. 8 The location of the strain gauge and the tension unit: (a) a single tension unit; (b) a dual tension 6 unit; and (c) no tension unit

Table 1 The peak load and corresponding strain for a general bolt without an active tension unit

Without a tension unit		Loose sand		Dense sand	
Surcharge	Location	Strain	Load (N)	Strain	Load (N)
60 Kg	L01	10.5	30.21	11.25	29.43
	L02	9	30.21	15	29.43
	L03	12.5	30.21	15.75	29.43
	L04	12	30.21	14.25	29.43
	L05	11.5	30.21	12	29.43
	L06	10.5	30.21	12	29.43
	L07	10	30.21	9.75	29.43
	L08	9	30.21	16.88	29.43
	R01	7.16	28.67	10.5	32.08
	R02	8.65	28.67	12.75	32.08
	R03	10	28.67	11.25	32.08
	R04	10.41	28.67	12.75	32.08
	R05	10	28.67	13.5	32.08
	R06	9.58	28.67	14.25	32.08
	R07	9	28.67	12.75	32.08
	R08	8	28.67	15.75	32.08
90 Kg	L01	11.49	29.2	8.12	30.9
	L02	10.5	29.2	10.5	30.9
	L03	12.83	29.2	8.5	30.9
	L04	10.5	29.2	7	30.9
	L05	11.2	29.2	7.5	30.9
	L06	11.9	29.2	9	30.9
	L07	12.6	29.2	8	30.9
	L08	13.24	29.2	6	30.9
	R01	11.49	28.81	8.12	32.76
	R02	10.5	28.81	10.5	32.76
	R03	12.83	28.81	8.5	32.76
	R04	10.5	28.81	7	32.76
	R05	11.2	28.81	7.5	32.76
	R06	11.9	28.81	9	32.76
	R07	12.6	28.81	8	32.76
	R08	13.24	28.81	6	32.76
120 Kg	L01	9.75	30.12	7.24	30.12
	L02	13.5	30.12	9.8	30.12
	L03	10.53	30.12	11.18	30.12
	L04	14.25	30.12	13.95	30.12
	L05	12.75	30.12	13.16	30.12

Table 1 Continued

Without a tension unit		Loose sand		Dense sand	
Surcharge	Location	Strain	Load (N)	Strain	Load (N)
120 Kg	L06	12	30.12	14	30.12
	L07	11.7	30.12	7.7	30.12
	L08	10	30.12	8.4	30.12
	R01	9	30.44	7.24	32.82
	R02	12	30.44	9.8	32.82
	R03	10	30.44	11.18	32.82
	R04	12	30.44	13.95	32.82
	R05	12	30.44	13.16	32.82
	R06	12.5	30.44	14	32.82
	R07	9.75	30.44	7.7	32.82
	R08	8.5	30.44	8.4	32.82

Table 2 The peak load and corresponding strain for active tension bolt with a single tension unit

Single tension unit		Loose sand		Dense sand	
Surcharge	Location	Strain	Load (N)	Strain	Load (N)
60 Kg	LL1	7.2	30.61	9	30.9
	LL2	6.4	30.61	6.75	30.9
	LL3	6	30.61	6.5	30.9
	LL4	5.6	30.61	5.5	30.9
	LL5	7.6	30.61	5	30.9
	LL6	6.9	30.61	5.5	30.9
	LL7	8.4	30.61	6.5	30.9
	LL8	6.8	30.61	6	30.9
	RL1	7.2	33.36	7.18	27.47
	RL2	6.4	33.36	6.75	27.47
	RL3	6	33.36	5.24	27.47
	RL4	5.6	33.36	5.63	27.47
	RL5	7.6	33.36	6	27.47
	RL6	6.9	33.36	6	27.47
	RL7	8.4	33.36	9	27.47
	RL8	6.8	33.36	8.19	27.47
90 Kg	LL1	7.18	27.47	5.1	30.31
	LL2	6.75	27.47	7.5	30.31
	LL3	5.63	27.47	4.67	30.31
	LL4	5.63	27.47	3.5	30.31
	LL5	6	27.47	5.45	30.31

Table 2 Continued

Single tension unit		Loose sand		Dense sand	
Surcharge	Location	Strain	Load (N)	Strain	Load (N)
90 Kg	LL6	6	27.47	5.2	30.31
	LL7	5.4	27.47	4.3	30.31
	LL8	8.33	27.47	3.05	30.31
	RL1	7.2	28.84	4.1	30.71
	RL2	7.65	28.84	5.5	30.71
	RL3	6.27	28.84	4.67	30.71
	RL4	5.52	28.84	5	30.71
	RL5	7.04	28.84	5.45	30.71
	RL6	6.75	28.84	4.5	30.71
	RL7	10.13	28.84	3.5	30.71
	RL8	8.25	28.84	6.05	30.71
120 Kg	LL1	5.56	24.72	8.3	28.65
	LL2	4	24.72	6.39	28.65
	LL3	4.54	24.72	5.3	28.65
	LL4	4.5	24.72	6.68	28.65
	LL5	5	24.72	5.88	28.65
	LL6	4.5	24.72	5.88	28.65
	LL7	3.85	24.72	6.5	28.65
	LL8	4.51	24.72	5.52	28.65
	RL1	5.99	24.23	8.3	31.79
	RL2	4.5	24.23	6.39	31.79
	RL3	4	24.23	5.3	31.79
	RL4	5.37	24.23	6.68	31.79
	RL5	4.5	24.23	5.88	31.79
	RL6	4	24.23	5.88	31.79
	RL7	6.3	24.23	6.5	31.79
	RL8	3.69	24.23	5.52	31.79

Table 3 The peak load and corresponding strain for the active tension bolt with a dual tension unit

Dual tension unit		Loose sand		Dense sand	
Surcharge	Location	Strain	Load (N)	Strain	Load (N)
60 Kg	LS1	4.29	28.65	2	30.12
	LS2	3.66	28.65	1.33	30.12
	LL9	4.24	28.65	1.33	30.12
	LL10	3.45	28.65	1.83	30.12
	LL11	4.84	28.65	1.67	30.12

Table 3 Continued

Dual tension unit		Loose sand		Dense sand	
Surcharge	Location	Strain	Load (N)	Strain	Load (N)
60 Kg	LL12	3.71	28.65	2	30.12
	LS3	4.24	28.65	1.17	30.12
	LS4	2.27	28.65	0.83	30.12
	RS1	4.29	31.04	1.83	30.92
	RS2	3.44	31.04	1.5	30.92
	RL9	3.63	31.04	1.5	30.92
	RL10	3.2	31.04	2	30.92
	RL11	3.98	31.04	1.5	30.92
	RL12	3.45	31.04	2.17	30.92
	RS3	3.71	31.04	1.33	30.92
	RS4	2.27	31.04	1	30.92
90 Kg	LS1	2.5	28.45	1.5	30.61
	LS2	3.67	28.47	1.12	30.61
	LL9	4.9	28.47	2	30.61
	LL10	3.82	28.47	2.2	30.61
	LL11	3.38	28.47	1.6	30.61
	LL12	2.5	28.45	1.71	30.61
	LS3	3.36	28.47	1.5	30.61
	LS4	3.05	28.47	1.4	30.61
	RS1	3.5	30.56	1.62	31.94
	RS2	3.7	30.56	2.01	31.94
	RL9	4.5	30.56	3.2	31.94
	RL10	3.2	30.56	1.42	31.94
	RL11	3.51	30.56	1.67	31.94
	RL12	2.38	30.56	1.7	31.94
	RS3	3.05	30.56	2.1	31.94
	RS4	2.03	30.56	2.11	31.94
120 Kg	LS1	2.5	34.63	1.12	29.24
	LS2	1.33	34.63	1.5	29.24
	LL9	2	34.63	3	29.24
	LL10	0.83	34.63	2.13	29.24
	LL11	1.83	34.63	1.5	29.24
	LL12	2.17	34.63	1.83	29.24
	LS3	2	34.63	1.5	29.24
	LS4	2	34.63	1.17	29.24
	RS1	2.5	448.91	1.12	31.87
	RS2	2.83	448.91	1.5	31.87

Table 3 Continued

Dual tension unit		Loose sand		Dense sand	
Surcharge	Location	Strain	Load (N)	Strain	Load (N)
120 Kg	RL9	2	448.91	3	31.87
	RL10	2.5	448.91	2.13	31.87
	RL11	2.83	448.91	1.5	31.87
	RL12	3.04	448.91	1.83	31.87
	RS3	2.49	448.91	1.5	31.87
	RS4	2.17	448.91	1.17	31.87

Table 4 Effects of the active tension bolt on the horizontal displacement of the pillar

Test	Without the active tension bolt			With the active tension bolt		
	Displacement on the left-hand side (mm)	Displacement on the right-hand side (mm)	Total (mm)	Displacement on the left-hand side (mm)	Displacement on the right-hand side (mm)	Total (mm)
Test 1	3.87	7.47	11.34	2.72	4.77	7.49
Test 2	3.52	7.57	11.09	2.41	3.98	6.39
Test 3	3.46	8.28	11.74	2.62	4.98	7.6

amplified frictional resistance, and therefore pullout resistance increased in dense sand. In the case of the active tension bolt with a single tension unit, an increase in the surcharge increased the modulus. However, the effect of the surcharge was not consistent in the other cases, implying no significant effect of the surcharge on the mobilization of the modulus but a significant effect of the initial density of ground.

The most significant factor affecting the modulus of the bolt was the number of active tension units. The case of a bolt without an active tension unit showed the lowest level of the modulus (MWO). An increase in the number of active tension units increased the modulus. The modulus of the active tension bolt with a single tension unit was twice MWO. In particular, if there are two active tension units in a single rod, then the modulus showed the maximum level about five times MWO. These results indicate that the use of the active tension bolt enhanced the performance of the support system.

(a)

Fig. 9 The test setup for the active tension bolt: (a) a single tension unit; (b) a dual tension unit; and (c) no tension unit

(b)

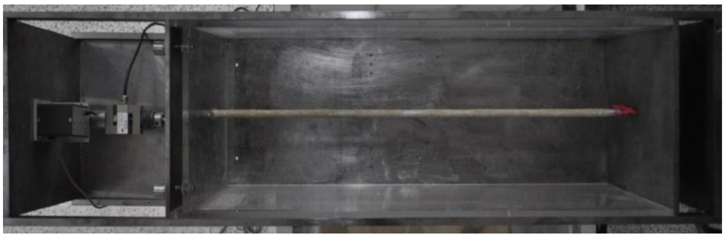

(c)

Fig. 9 Continued

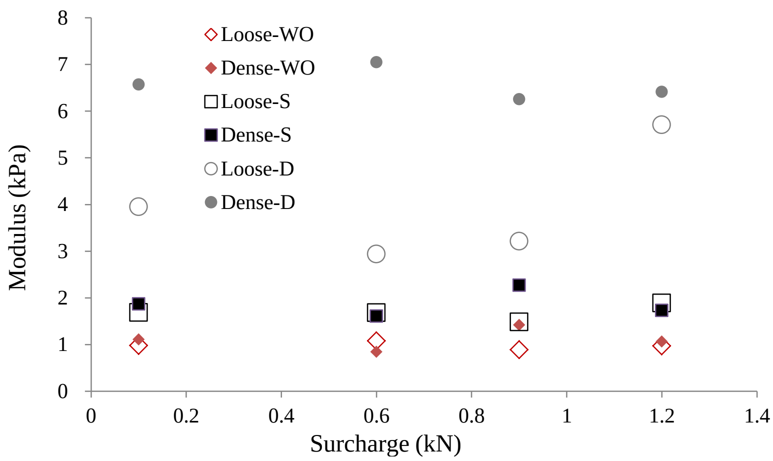

Fig. 10 Changes in the modulus from the number of active tension units under a surcharge in loose and dense sand (Note: WO, S, and D denote bolt without active tension unit, bolt with single active tension unit, and bolt with dual active tension units, respectively)

4. The application of the active tension bolt to pillar reinforcement

4.1 The reinforcing mechanism

Peck (1969) reports the distortion induced by the parallel construction of twin tunnels and suggests that the distortion of an existing tunnel from the excavation of a nearby tunnel is governed by the width and depth of pillars, the main factors influencing the interaction between closely located tunnels. Based on Kim *et al*. (2012), the portion of some displacement induced by tunnel excavation at the same level is less than 10% if the pillar width exceeds the tunnel diameter. However, this effect can be influenced by the in situ stress and strength of the ground. Therefore, the stability evaluation of the existing tunnel in the context of a nearby tunnel should be carefully examined, and Peck's guidelines may be used in the initial design stages of the parallel construction of twin tunnels.

The average stress (S_p) at the tunnel pillar can be approximated as follows

$$S_p = \gamma H \left(1 + \frac{B}{\omega}\right) = \sigma_0 \left(1 + \frac{1}{\omega/B}\right) \tag{2}$$

where γ is the unit weight, H is the tunnel depth, B is the tunnel width, and ω is the pillar width. Schematic diagram is presented in Fig. 11(a).

The uniaxial compressive strength of the pillar (σ_p) can be estimated as follows

$$\sigma_p = \frac{2c \cdot cos\phi}{1 - sin\phi} \tag{3}$$

where c is cohesion and ϕ is the friction angle.

Therefore, the safety factor of the tunnel pillar against the initial yield can be defined as follows

$$\mathrm{FOS} = \frac{\sigma_p}{S_p} \tag{4}$$

The relationship between the ratio of the pillar width to the tunnel width (ω/B) and that of pillar strength to vertical stress (σ_p/σ_0) according to the safety factor can be obtained using Eqs. (2)-(4) and shown as in Fig. 11(b). This chart is useful for determining the width of the tunnel pillar from the strength and vertical stress of the tunnel pillar.

According to the design principal for the tunnel pillar width, the pillar stress (S_p) should be less than pillar strength (σ_p) after the pillar yield. If the pillar is weak and cannot satisfy the aforementioned condition, then the support system design of the tunnel pillar needs to refer to an

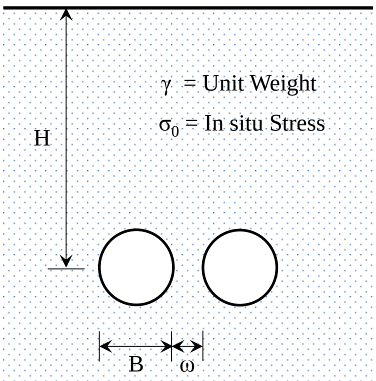

(a)

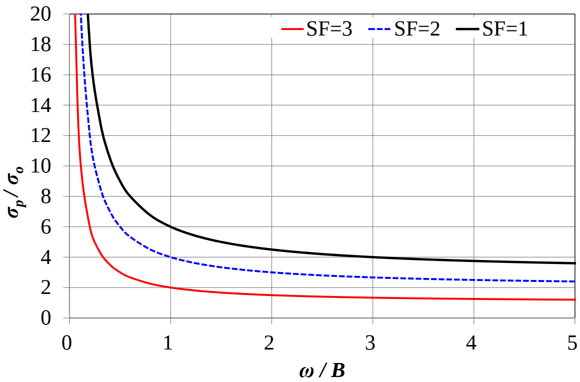

(b)

Fig. 11 Design of tunnel pillar: (a) Schematic diagram; (b) Effects of the safety factor on the relationship between ω/B and σ_p/σ_0

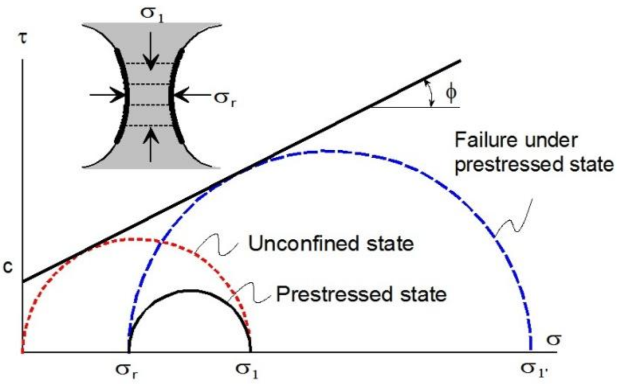

Fig. 12 Changes in the Mohr circle from pillar reinforcement

observational analysis, not to an empirical design standard. In general, a guaranteed pillar reinforcement method is to increase pillar strength by using the active tension bolt. The introduction of pre-stress with the active tension bolt can increase pillar strength.

If the active tension bolt introduces pre-stress to the tunnel pillar, then the strength of the tunnel pillar changes from a uniaxial compression state to a triaxial one. Therefore, pillar strength (σ_p) increases enough to support pillar stress (S_p). In this regard, based on the design principal of the active tension bolt for a tunnel pillar, if the in situ stress is σ1, then the pillar stress can be increased from 0 to σ_r through pre-stress, as shown in Fig. 12.

The design process of the tunnel pillar with the active tension bolt can be described as follows: First, the average stress of the tunnel pillar can be derived from Eq. (2). Second, the uniaxial compressive strength of the pillar can be derived from cohesion and friction angles based on Eq. (3). Finally, the deficient strength of the pillar can be determined using the predefined safety factor based on Eq. (4). Here pre-stress is calculated to make the minimum principal stress for σ_1 based on Figs. 11-12.

4.2 The experimental test and results

Fig. 13 shows the experimental setup for investigating the performance of the active tension bolt for pillar reinforcement. Three active tension bolts were installed in 10 cm intervals at the center of a pillar fabricated with an acryl plate 1 cm thick (30 cm in width, 40 cm in height, and 50 cm in depth). LVDTs were installed to measure the horizontal displacement at each wall. Two types of test sets were considered: a tunnel pillar with the active tension bolt and that without. Therefore, a total of six tests were conducted to investigate the performance of the active tension bolt for pillar reinforcement. The vertical load was gradually applied to the top of the specimen until it reached 80 kg. Table 4 tabulates the test results.

As a result, an increase in the stress produced a significant increase in the displacement at the wall on the right-hand side when there was no active tension bolt in the pillar. However, the lateral displacement increased gradually with an increase in the stress when the pillar was reinforced with the active tension bolt. As shown in Table 4, the total wall displacement for the case without the active tension bolt and that for the case with the active tension bolt were 11.39 mm and 7.16 mm, respectively. That is, 37.1% of the displacement could be reduced by using the active tension bolt. This implies the ability of the active tension bolt to reinforce the tunnel pillar.

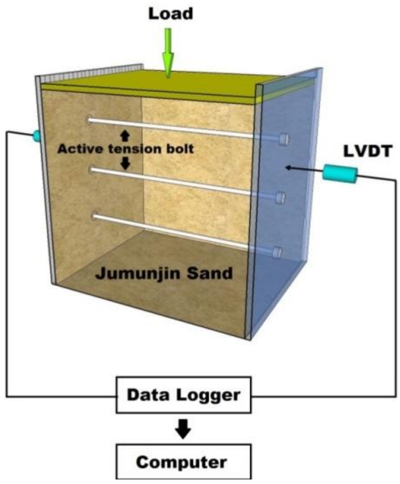

Fig. 13 The experimental setup for investigating the performance of the active tension bolt for pillar reinforcement

5. Conclusions

This paper proposes an innovative support system that can actively reinforce the weak ground along the whole structural element. More specifically, the paper introduces an active tension bolt containing a spring unit in the middle of the steel bar to increase the reinforcement capacity, presents the support mechanism of the active tension bolt based on a theoretical study, and considers an experimental study to evaluate the performance of the proposed active tension bolt. In addition, the paper employs a pullout test and a small-scale experimental model to examine the suitability of the active tension unit for tunnel pillars. The experimental results suggest that the active tension bolt can be an effective support system for tunnel pillar reinforcement.

The active tension bolt can secure the long-term stability. The tensile force can be released after a failure of the anchor system in a mechanical anchor bolt because the tensile force is supported and sustained only by the anchor at the end of the bolt. In the active tension bolt, however, the tensile force can be maintained even after a failure of the anchor at the end of the bolt because the local tension unit is embedded and fixed with grout. Therefore, a local failure induced by a fracture opening or a debonding interface induced by corrosion cannot affect the overall stability of the bolted section with the active tension bolt.

Various materials could be incorporated using the active tension bolt for particular purposes. For example, Glass-reinforced plastic (GRP) or fiber-reinforced plastic (FRP) can be used as support materials. These materials are more brittle than steel, and therefore, the removal of GRP and FRP bolts is much easier than that of a steel bolt when it is applied to tunnel face stabilization. GRP and FRP are clearly weak against shear, and therefore the application of GRP and FRP should be limited to support against the axial force.

As demonstrated in this paper, the active tension bolt can be used to reinforce pillars. The active tension bolt can be applied to slope stabilization and used as a rock bolt system in tunnels. In a shallow tunnel, the ground can be reinforced using the active tension bolt before excavation, and the active tension bolt can be implemented in various geotechnical fields to stabilize geotechnical infrastructures.

Acknowledgments

This research was supported by a grant (13SCIP-B066321-01) from the Construction Technology Research Program funded by the Ministry of Land, Infrastructure, and Transport of the Korean government. The study was supported by the INHA University and Hoseo University Research Grant. Hankook 2 Arch also support this research project.

References

ACI 349-79 (1976), Code requirements for nuclear safety related concrete structures, American Concrete Institute, Detroit, MI, USA.

AISC (2006), Steel Design Guide, Base plate and anchor rod design.

Ansell, A. (2005), "Laboratory testing of a new type of energy absorbing rock bolt", *Tunn. Undergr. Space Technol.*, **20**(4), 291-300.

Blanco-Fernandez, E., Castro-Fresno, D., Del Coz Diaz, J.J. and Lopez-Quijada, L. (2011), "Flexible systems anchored to the ground for slope stabilisation: Critical review of existing design methods", *Eng. Geol.*, **122**(3-4), 129-145.

Blanco Martín, L., Tijani, M. and Hadj-Hassen, F. (2011), "A new analytical solution to the mechanical behaviour of fully grouted rockbolts subjected to pull-out tests", *Construct. Build. Mater.*, **25**(2), 749-755.

Chappell, B.A. (1989), "Rock bolts and shear stiffness in jointed rock mass", *J. Geotech. Geoenviron. Eng.*, **115**(2), 179-197.

Chen, Y.J., Wu, H.W., Marcos, M.C.M. and Lin, S.S. (2013), "Improvement of tip analysis model for drilled shafts in cohesionless soils", *Geomech. Eng., Int. J.*, **5**(5), 447-462.

Delhomme, F., Debicki, G. and Chaib, Z. (2010), "Experimental behaviour of anchor bolts under pullout and relaxation tests", *Construct. Build. Mater.*, **24**(3), 266-274.

Divi, S., Chandra, D. and Daemen, J. (2011), "Corrosion susceptibility of potential rock bolts in aerated multi-ionic simulated concentrated water", *Tunn. Undergr. Space Technol.*, **26**(1), 124-129.

Eurocode 3 (2005), Design of steel structure – Part 1–8: Design of joints, European Standards, CEN, Brussels, Belgium.

Franzius, J.N., Potts, D.M., Addenbrooke, T.I. and Burland, J.B. (2004), "The influence of building weight on tunnelling-induced ground and building deformation", *Soil. Found.*, **44**(1), 25-38.

Jiang, S.H., Li, D.Q., Zhang, L.M. and Zhou, C.B. (2014), "Time-dependent system reliability of anchored rock slopes considering rock bolt corrosion effect", *Eng. Geol.*, **175**, 1-8.

Kim, D.K., Oh, B.J. and Lee, S.D. (2009), "Optimal pillar width of twin tunnels in horizontal jointed rock", *ITA-AITES World Tunnel Congress2009*, Budapest, Hungary, May.

Komurlu, E. and Kesimal, A. (2015), "Sulfide-rich mine tailings usage for short-term support purposes: An experimental study on paste backfill barricades", *Geomech. Eng., Int. J.*, **9**(2), 195-205.

Lee, I.M., Han, S.I., Kim, H.J., Yu, J.D., Min, B.K. and Lee, J.S. (2012), "Evaluation of rock bolt integrity using Fourier and wavelet transforms", *Tunn. Undergr. Space Technol.*, **28**(1), 304-314.

Li, C. and Stillborg, B. (1999), "Analytical models for rock bolts", *Int. J. Rock Mech. Min. Sci.*, **36**(8), 1013-1029.

Liu, X.R., Li, D.L., Wang, J.B. and Wang, Z. (2015), "Surrounding rock pressure of shallow-buried bilateral bias tunnels under earthquake", *Geomech. Eng., Int. J.*, **9**(4), 427-445.

Livaoglu, R. (2013), "Soil interaction effects on sloshing response of the elevated tanks", *Geomech. Eng., Int. J.*, **5**(4), 283-297.

Mahdi, M. andKatebi, H. (2015), "Numerical modeling of uplift resistance of buried pipelines in sand, reinforced with geogrid and innovative grid-anchor system", *Geomech. Eng., Int. J.*, **9**(6), 757-774.

Osgoui, R.R. and Ünal, E. (2009), "An empirical method for design of grouted bolts in rock tunnels based on the geological strength index (GSI)", *Eng. Geol.*, **107**(3), 154-166.

Peck, R.B. (1969), “Deep excavations and tunnelling in soft ground”, *Proceeding of the 7th International Conference on Soil Mechanics and Foundation Engineering*, Mexico City, Mexico, pp. 225-290.

Pells, P. and Bertuzzi, R. (1999), “Permanent rockbolts - The problems are in the detail”, *Proceeding from 10th Australian Tunnelling Conference*, Melbourne, Australia, March.

Petros, P. (1991), *Ground Anchors and Anchored Structures*, John Wiley and Sons, Canada.

Siad, L. (2001), “Stability analysis of jointed rock slopes reinforced by passive fully grouted bolts”, *Comput. Geotech.*, **28**(5), 325-347.

Song, K.I., Cho, G.C., Chang, S.B. and Lee, I.M. (2013), “Beam-spring structural analysis model for the design of tunnel pre-reinforcement support system”, *Int. J. Rock Mech. Min. Sci.*, **59**, 139-150.

Song, M.K., Choo, S.Y., Kang, S.S. and Cho, Y.D. (2010), “A supportability comparison of rock and spiral bolts with numerical method”, *Proceedings of the Regional Symposium of the International Society for Rock Mechanics EUROCK 2009*, Dubrovnik, Croatia, October, pp. 679-684.

Spearing, A.J.S., Greer, B. and Reilly, M. (2011), “Improving rockbolt installations in US coal mines”, *J. South Afr. Inst. Min. Metallurgy*, **111**(8), 555-563.

Zhao, Y.C., Zhang, J.Y. and Xiang, Z.Q. (2013), “Research on arching mechanism of the lane arching under pre-stress bolt supporting”, *Adv. Mater. Res.*, **671-674**, 1140-1143.

GC